JOURNAL OF FIRE SCIENCES

Original Research Article

Journal of Fire Sciences
2024, Vol. 42(5) 439–469

DOI: 10.1177/07349041241237536
journals.sagepub.com/home/jfs
Sage

Durability and performance of wood flour/polyethylene composites containing fire retardants after weathering via ASTM D2565

Mark Anthony Dietenberger, Nicole M Stark and Charles Boardman

Date received: 28 August 2023; accepted: 20 February 2024

Abstract

Wood–plastic composites are composite materials consisting of wood particles, thermoplastic polymer, and small amounts of other performance additives to increase performance in exterior construction applications such as decking and siding. Three best-performing fire retardants, determined from a previous study, which were brominated, magnesium hydroxide, and ammonium polyphosphate, were selected for this weathering study and more detailed analysis with color analysis, thermogravimetric analysis/differential scanning calorimetry, and the cone calorimeter. With the rapid surface heating condition at cone calorimeter irradiance of 50 kW m^{-2}, modest surface leaching of fire retardant was detected as caused by weathering via increased first peak heat-release rate and reduced time to ignition values. Otherwise, the weathering had minimal effect on the remaining heat-release rate profile, and results confirmed ammonium polyphosphate as top performing fire retardant, even better than Ipe wood, with magnesium hydroxide and brominated slightly worse than Ipe. This suggests that 35% high-density polyethylene content reduced fire retardant bulk leaching.

Keywords

Wood–plastic composite, fire retardants, mechanical properties, heat release rate, accelerated weathering

USDA Forest Products Laboratory, Madison, WI, USA

Corresponding author:
Mark Anthony Dietenberger, USDA Forest Products Laboratory, Madison, WI 53726, USA.
Email: mark.a.dietenberger@usda.gov

Introduction

Wood–plastic composites (WPCs) are composite materials consisting of wood particles, thermoplastic polymers, and small amounts of other additives to increase performance or processability.[1] WPCs are important in several markets including consumer products, automotive, and construction applications with building and construction accounting for more than 71% of global revenue share in 2022.[2]

The use of WPCs as decking and railing systems continues to grow due to the advantage of being more resistant to moisture, insects, decay, and warping when compared to traditional pressure-treated lumber which can result in lower maintenance requirements. To continue growth in exterior applications, WPCs must be a durable material with resistance to moisture, biodeterioration, weathering, and fire. For further expansion into the construction market, understanding the flammability of WPCs and improving fire retardancy is of great interest.

Fire performance of WPCs

The fire performance of WPCs depends upon the polymer type, wood concentration, and use of additives. Generally, the fire performance of WPCs falls between the performance of unfilled plastic and solid wood materials. Early studies compared WPCs produced commercially and in a laboratory with solid wood and neat polyethylene (PE). Heat-release rate (HRR) results based on cone calorimeter data established that WPCs demonstrated better fire performance than neat polymer, but worse than solid wood.[3,4] However, the ignition time (IT) of WPCs was similar to solid wood and lower than PE. The results suggested that although it took longer for PE to ignite compared with wood, once ignition was underway PE released more heat and combustion consumed the material faster than wood. For WPCs, it is uncertain whether the fibers act as a wick for the melted thermoplastics, or that the fibers themselves pyrolyze sufficiently to provide fuel for ignition. As the concentration of wood in WPCs increases, the fire performance of WPCs also improves. One early study compared WPCs containing 20% or 50% wood content in polypropylene (PP) or high-density polyethylene (HDPE) matrices determined the HRR of composites containing 20% wood was significantly higher than composites containing 50% wood fiber.[4] One strategy to reduce the intensity of burning is therefore to increase the wood content of the WPC.[5] The properties of the plastic can also impact fire performance. For example, one study reported that cone calorimeter results indicated that the PP-based WPCs had longer IT, lower HRR, and longer total burning time as melt-flow index of PP increased.[6] The observations were interpreted as being connected to variations in the wettability of the particles of the wood by the plastic.

Improving the fire performance of WPCs is commonly accomplished by adding additive-type fire retardants (FRs) into the plastic matrix during processing. Additive-type FRs come in many forms, although most are particles or powders. Effective additive-type FRs for WPCs include metal hydroxides (aluminum hydroxide or magnesium hydroxide (MH)), zinc borate, ammonium polyphosphate (APP), and halogenated species such as organochlorine and organobromine.[7–15] Halogenated FRs are less commonly used due to the release of toxic compounds upon thermal degradation. Additive-type FR improves fire performance through the following mechanisms: (1) release of reactive-free radicals that react with decomposed combustible radical substances to retard flame development, (2) release non-flammable compounds such as water and inert gases that reduce temperature and dilute fuel

supply, (3) formation of char layer and/or foaming compound that act as thermal insulation and partial thermal absorbers separating the bulk material from the gas phase,[8] and (4) incorporation in the bulk materials that improve the heat sink effect via higher heat of gasification and higher specific heat.[10]

Studies evaluating fire performance of WPCs have shown that fire performance can be improved through the addition of each of these FRs into the plastic matrix to various degrees. The reported effectiveness of metal hydroxides in WPCs has been mixed. Sain et al.[9] reported an improvement in oxygen index with the incorporation of MH while Abu Bakar et al.[14] reported no positive effect on fire retardancy with the addition of MH. In some studies, MH can be up to 30% of the total composite when used as an FR.[10] In this study, limited oxygen index was improved, but it is difficult to determine if that was due to the addition of MH, reduction in polymer content, or a combination of the two. Boron-based compounds in the form of zinc borate have been studied primarily as a partial substitution for other FRs. For example, a partial replacement of MH with zinc borate decreased oxygen index, lowering fire performance.[9] Another effort found that partial substitution of a bromine-based FR with zinc borate resulted in an increase in fire performance, while partial substitution of a phosphorous-based compound with zinc borate decreased WPC fire performance.[11] Although combinations of zinc borate with other phosphate-based FRs can decrease HRR of WPCs, in some cases observed improvements may also be partly due to displacing the polymer matrix with FRs.[12]

Most research investigating FRs for WPCs has focused on phosphorous-based compounds. Comparisons between APP and melamine phosphate showed that APP was more effective at increasing oxygen index of WPCs.[13] Others have also reported positive effects of fire retardancy with the incorporation of APP.[11,14,15,16] APP can be combined with other flame retardants to improve the efficacy. A novel flame-retardant system for WPCs based on the combination of APP with phytic acid modified layered double hydroxide showed improved char formation, which resulted in higher fire resistance.[17] Combining APP with silicon dioxide nanofillers also provide synergistic FR retardant action in WPCs.[18,19] Halogenated compounds based on bromine, used in combination with antimony oxide have been proven effective at improving the oxygen index of WPCs.[11]

It can be challenging to directly compare fire performance of WPCs and identify which FRs are best for WPCs because the WPCs use different matrix materials, wood species, wood contents, and test methods. There have been studies that directly compare the efficacy of different FRs for WPCs. One study compared APP, MPP, and aluminum hydroxide added to PP-based WPCs. It was reported that the lowest peak HRR was obtained when APP was added, but the lowest total HRR occurred for WPCs containing aluminum hydroxide.[20]

In a study comparing fire performance containing MH, APP, BR FR, and zinc borate (all 10% by weight), it was determined that WPCs containing either MH or APP performed the best.[21]

There has been some research in protecting WPC by treating the wood component with FRs prior to compounding with the thermoplastic rather than adding FRs to the composite during processing. In one study, wood particles from FR-treated particleboard combined with thermoplastics demonstrated improved performance.[22] Related studies demonstrated that APP was effective as an FR when the wood component was treated prior to combination with the thermoplastic.[22] In a related study, various FRs were used to pre-treat wood flour (WF) prior to combination with plastics. In a two-step process, the materials were combined, exposed to water, and then formed into the final shape. The aim of the study was to

evaluate how much FR leached out when exposed to water during manufacturing. In general, low amounts of phosphorus leaching were observed during processing. Pre-treatment of the wood with FR also resulted in less water uptake compared with adding FR to the bulk of the composite.[23]

Weathering of polymers results in changes such as surface cracking, chain scission, and photooxidation primarily due to ultraviolet (UV) exposure. It has been well established that this can impact the performance of plastics containing FRs.[24,25] Weathering the surface of WPCs can lead to changes in the polymer structure due to UV exposure, and also microcracks and surface erosion due to water exposure.[26] As a result, when exposed to exterior environments, FR systems in WPCs may lose efficacy due to leaching or negative interactions with other additives that improve durability. In one study, adding FRs to WPCs worsened outdoor durability. However, when the FRs were added with a light stabilizer, both fire retardancy and outdoor durability were improved.[13] The fire retardancy of WPCs can also decrease after weathering, and in some cases, this may result in a WPC passing a certain classification before weathering but failing after weathering.[27] Therefore, it is critical to systematically evaluate the fire performance of WPCs before and after weathering.

Objectives of this study

The objective of this study is to (1) determine any degradation due to accelerated weathering for the fire and mechanical properties of the best-performing fire retardant treatment WPCs reported in our earlier study[21] and (2) provide insights into the mechanisms of operation from additional testing and data analysis with thermogravimetric analysis/differential scanning calorimetry (TGA/DSC) and color measurements. At the bench scale, we used the weathering protocol of ASTM D2565, *Standard Practice for Xenon-Arc Exposure of Plastics Intended for Outdoor Applications*, in conjunction with cone calorimeter testing to determine any degradation in fire performance. Discussion of the additional TGA/DSC results suggests the mechanisms by which the FR influences the cone calorimeter HRR results. Finally, by modeling the Stefan basis of charring,[28] we sort the FR mechanisms as to their importance in reducing the HRR of the base WPC as exposed to 50 kW m^{-2} irradiances with piloted ignition condition in the cone calorimeter.

Experimental methods

Materials and manufacturing method

The base WPCs investigated consisted primarily of PE and WF. The PE had a melt flow index of 5 and was purchased from ExxonMobil (HD 6605.70, Houston, TX). American Wood Fibers supplied 40 mesh, mixed pine WF (AWF 4020, Schofield, WI). To maintain good composite surface characteristics, a lubricant was added to each composite. Struktol Company of America supplied the lubricant (TPW 113, Stow, OH). In addition, three additive-type FR systems were investigated for accelerated weathering process:

1. Decabromodiphenyl oxide (BR) (Saytex 102E, Albemarle Corporation, Baton Rouge, LA) and antimony trioxide (AT) (BrightSun HB, China Antimony Chemicals Co., Ltd., Guangxi, China)
2. MH (Magnifin H-10, Albemarle Corporation, Baton Rouge, LA)
3. APP (Exolit AP 422, Clariant Corporation, Charlotte, NC)

The formulations examined are shown in Table 1. Composites without FRs had 60% by weight WF, while composites with FRs incorporated 50% WF and 10% of the FR system. Based on results from our previous study,[21] this formulation allows WPC to be compared based on consistent PE content (35%) while maintaining mechanical properties associated with the relatively high WF content. This meant relying on no more than 10% FR while utilizing their synergistic features to achieve the needed fire performance after weathering. Because these WPC had relatively high WF contents that inherently improved their fire performance along with the better mechanical properties,[21] we are able to avoid the relatively high FRT content in thermoplastics associated with other applications, such as wire cables,[29–31] to achieve the appropriate fire performance. With the focus on structural uses of the WPC, one will want to avoid the HDPE melting at 135°C on the fire unexposed region of the product, meaning that charring or intumescent on the exposed region to reduce heat flux within the low-density degraded material will be desirable. For example, the APP additive is known to enhance charring at low concentrations, and promote intumescent at high concentrations, but the high concentrations of APP are avoided here to maintain mechanical properties due to the high WF content. We also avoid leach-resistant flame-retardant treatments for wood based on a reaction product of phosphoric acid with urea-formaldehyde and dicyandiamide resin[32] because of the desire for minimal changes to the manufacturing process and keeping such products more affordable, simpler, and renewable.

A 32-mm Davis Standard (Pawcatuck, CT) twin-screw co-rotating extruder combined with a Schenck AccuRate (Whitewater, WI) loss-in-weight feeder system was used for all compounding. The barrel of the extruder had 10 separate zones, with zones 4 and 9 vented to the atmosphere. The screw had a 36:1 L/D ratio consisting primarily of conveying elements, with kneading and mixing elements incorporated into the screw before the vents to build up pressure and disperse and mix the components. The extruder was outfitted with a strand die; the strand extrudate was cooled in a water slide and pelletized. The composites were compounded in two steps. In the first step, PE was compounded with wood fiber, lubricant, and FR as shown in Table 1. For the specimens with FR, compounding ensured thorough incorporation of the FR. The melt temperature ranged from 192°C to 201°C, while the melt pressure ranged from 3.6 to 4.5 MPa. Prior to the second compounding step, WF was dried for 24 h at 105°C. The dried WF was then compounded with lubricant and the already compounded PE with or without FR as shown in Table 1. During the second compounding step, the melt temperature ranged from 188°C to 199°C suitable for HDPE while the melt pressure ranged from 4.2 to 7.0 MPa. It is possible during the melting and compounding that some of the FR has dissolved and percolated with the PE into the WF. To avoid WF degradation at the melt temperature the time duration of the second compounding step was kept

Table 1. Formulations of WPCs manufactured with fire retardants

	Composition based on weight (%)						
Code	PE	WF	BR	AT	MH	APP	Lubricant
WF-60	35	60					5
WF-BR	35	50	7.5	2.5			5
WF-MH	35	50			10		5
WF-APP	35	50				10	5

short. The melt temperature of up to 199°C also requires the FR to not be active nor degrading while compounding. These restrictions along with the needed favorable mechanical and environmental properties with only 10% FR content led to the three feasible FR products for this study related to their weathering.

To form composite boards for cone calorimeter testing, the compounded pellets were dried at 105°C for at least 24 h before being processed into boards using a Davis Standard 89-mm single-screw extruder (Pawcatuck, CT). The melt temperature ranged between 167°C and 174°C. The extrudate was formed using a 13.5 mm × 127 mm radius-edge profile die.

Accelerated weathering

Procedures for establishing WPC performance ratings in North America are found in ASTM D7032, Establishing Performance Ratings for Wood–Plastic Composite and Plastic Lumber Deck Boards, Stair Treads, Guards, and Handrails.[33] According to this procedure, typical weathering tests are ASTM D2898, Standard Practice for Accelerated Weathering of Fire-Retardant-Treated Wood for Fire Testing[34] and ASTM D2565, Standard Practice for Xenon-Arc Exposure of Plastics Intended for Outdoor Applications[35] for wood and plastics, respectively. In this study, WF-HDPE composites were placed in a xenon arc–type light exposure apparatus operated according to ASTM D2565 (Ci5000, Atlas Weathering, Chicago, Illinois). Samples were mounted on a drum that rotates around a xenon arc bulb at 1 r/min. Each 2-h weathering cycle consisted of 108 min of UV exposure and 12 min of simultaneous water spray and UV exposure. The samples were exposed for 2000 h. The average irradiance was 0.70 Wm^{-2} at 340 nm wavelength. The test lamp was calibrated every 400 h of irradiation, and the inner filter of the test lamp was changed simultaneously.

TGA/DSC measurements

Extending the insights offered for the pure HDPE with the APP FR by Schirp and Schwarz,[27] the HDPE composites were tested in Mettler-Toledo TGA/DSC 3+ using the heating rate of 7°C min^{-1} and standard TGA aluminum pan with a pinhole cover. Although much of the literature consider an alumina pan with a heating rate of 10°C min^{-1}, we follow the manufacturer's recommendation for the optimized use of the combined TGA and DSC measurements using the same pan. Besides, our intention is to obtain results that are relevant to the cone calorimeter fire testing, rather than comparing with literature results on the use of the TGA. The samples retrieved from the accelerated weathering apparatus had a lighter-in-color front side that was exposed to UV and water and a rear side that was exposed to only the water that retained its color. An electric saber saw was used to obtain thin ~1-mm slabs from the front and rear sides of the sample and round button specimens were obtained with a leather hole puncher. Each sample button fit snugly in the aluminum pan. The degradation mass loss and heat of pyrolysis properties of WF and HDPE components as a function of temperature were determined. The wood, with its charring temperature around 300°C and negligible overall heat of reaction for pyrolysis[36,37] offers the char as an insulation and substrate for the adhering melted HDPE. In contrast, the higher temperature pyrolysis of the melted HDPE at ~475°C involves high heat of pyrolysis and high heat of combustion (LHV = 45 kJ g^{-1}) of its volatiles, which are mainly ethylene.[38] The use of aluminum pan limited the maximum temperature to 595°C, and the furnace provided either N_2 gas or air flows. Given the high effectiveness of the TGA/DSC instrument and the

effectively good homogeneous samples, we found the replicate testing were not necessary to achieve the goals of this study.

Color measurement

A Minolta CR-200 Chroma Meter (Minolta Corporation, Ramsey, NJ) was used to measure color using the CIELAB color system.[39] In the CIELAB color system, the value L can be thought of as a lightness factor. L represents reflectance of a sample. An L^* of 0 means the sample does not reflect light; an L^* of 100 means the sample reflects 100% light. An increase in L^* means the sample has faded or "lightened." Measurements were taken at six locations per sample, and for four replicate samples of each formulation. The measures a* and b* represent the color coordinates which range in value between +256 and –256 with a* representing red/green and b* representing yellow/blue with a value. The color difference, ΔE_{ab}, was determined using the procedure outlined in ASTM D2244, *Standard Practice for Calculation of Color Tolerances and Color Differences from Instrumentally Measured Color Coordinates*[39] (equation (1)).

$$\Delta E_{ab} = \left(\Delta L^2 + \Delta a^2 + \Delta b^2\right)^{1/2} \tag{1}$$

Fire performance tests

Cone calorimetry was performed on an Atlas Cone 2 Combustion Analysis System (Atlas Electrical Devices, Chicago, IL) according to ASTM E1354, *Standard Test Method for Heat and Visible Smoke Release Rates for Materials and Products Using an Oxygen Consumption Calorimeter*.[40] WPC samples were cut from the extruded boards to a size of 100 mm × 100 mm. The sample thickness was as extruded, at 13.5 mm. Samples were exposed in the horizontal orientation with the conical radiant electric heater located 25 mm above the specimen and the retainer frame (without the wire grid) over the test specimen. The sides and bottom of the samples were wrapped in aluminum foil. Each sample rested on an insulation fiber blanket to keep it apart from the holder during the test. A spark igniter started the burning process and the length of time required to create a steady flame (IT) was recorded. Three replicate samples, pre-weathered and post-weathered, were tested at a heat flux level of 50 kW m^{-2}. The exhaust system flow rate was 0.024 m^3 s^{-1}. Data collection for WPCs was stopped once the mass loss rate (MLR) dropped below 1.5 gm^{-2} s^{-1}. The WPCs ceased burning once the heat from the cone was removed. For reference, white pine (*Subgenus Strobus*) and Ipe (*Handroanthus*) boards cut to 100 mm × 100 mm by 12.7 mm were also subjected to fire performance testing. For another reference, the WPC samples were burned in a similar calorimeter apparatus (known as Mass Loss Calorimeter, ASTM E2102, *Standard Test Method for Measurement of Mass Loss and Ignitability for Screening Purposes Using a Conical Radiant Heater*)[41] with tiny thermocouples attached to the top and bottom of the samples via insertion in thin surface crevices in their centers and using similar test protocol described for the cone calorimeter. The intent was to compare the time evolution of specimen surface temperatures to that of the TGA/DSC to infer mass loss processes in the WPC panels exposed to 50 kW m^{-2} irradiances.

The primary output from the cone calorimeter test is an HRR versus time curve. HRR is defined as the heat evolved from the specimen per unit time and is determined by the oxygen consumed during burning.[40] Ignitability was determined by observing the time for sustained

ignition of the specimen and is reported as IT. For reporting purposes, the heat release curve was reduced to single numbers via the recorded initial peak HRR and calculated averages of the HRR over a set time (60 s, 300 s, and over the test duration) after ignition of the specimen was observed. The total heat release (THR), that is, the cumulative heat release over the duration of the test, the average MLR, and average effective heat of combustion (EHOC) for the test duration were also calculated according to ASTM E1354.[40] The different mechanisms of FRs can potentially be exploited to target their exterior use, based on the anticipated mode of attack from wildfires (i.e. radiation or embers, or both) and intensity. For example, an increased critical heat flux for ignition or IT could reduce the probability of wood igniting under lower intensity fires. Alternatively, reducing the HRR from wood once ignited, decreases the risk of flame spread along the burning front to other wooden elements. This is the impetus behind limiting the use of materials based on HRR as is done in both the Australian Standard AS 3959 *Construction of Buildings in Bushfire Prone Areas*[42] and California State Fire Marshall (SFM) 12-7A-4: *Materials and Construction Methods for Exterior Wildfire Exposure*[43] with limits of 100 kW m^{-2} and 269 kW m^{-2}, respectively. Here, we identify a different HRR criteria for the WPC materials evaluated based on the comparison to the Ipe wood.

Statistics

Also reported are bar graphs of the mean of the cone calorimeter data sets with error bars representing one standard deviation. To determine significant differences between compared means, two-sample t tests were carried out at $\alpha = 0.05$. Tests for significance were two-tailed and assumed normal distribution and equal population variances. The letters above each bar in these figures denote significance. If the letters are the same, the hypothesis that the difference between means is zero was accepted. Conversely, different letters denote that the difference between means is not zero, that is, the differences are statistically significant.

Results and discussion

Physical properties

The previous work evaluated, separately, the effect of weathering and FR additives on physical properties of WPC.[44,45] This study combines the previous studies by focusing on the effect weathering has on flammability of WPCs containing the best-performing FR. If FR is distributed uniformly throughout the bulk of a WPC, then the erosion of the surface by exposure to UV and water would have minimal effect on the inherent flammability. However, combined UV and water exposure has been shown to result in lightening of WPC surfaces and can lead to loss of strength and potential leaching of the FR from the surface.[44] Table 2 provides the ΔE_{ab} values with standard deviation for the FRT WPC post-weathering. The values indicate considerable lightening of the surface and similar ΔE_{ab} values to those previously measured for untreated WPC.[44] The WPC with BR and MH treatments resulted in relatively less lightening than that of the APP treatment. These results signify that, regardless of the FRs being used, the end-product will need UV stabilizer at least in the surface layer to preserve the WPC coloring. The lightening appears in some depth to about 2 mm, enough to provide thin 1 mm surface layer samples via the cut and punch method for the TGA/DSC observations.

Table 2. Effect of weathering on surface coloring of FRT WPC

	Before weathering			After weathering			ΔE_{ab}
	L*	A*	B*	L*	A*	B*	
WF-60	54.9 (0.4)	8.18 (0.2)	21.8 (0.2)	93.0 (0.06)	−0.03 (0.08)	2.4 (0.3)	43.5 (0.4)
WF-BR	63.5 (0.4)	6.62 (0.03)	21.1 (0.2)	94.6 (0.3)	−0.09 (0.07)	3.8 (0.5)	36.3 (0.2)
WF-MH	60.0 (0.7)	6.80 (0.4)	21.4 (1.4)	89.6 (3.9)	−0.09 (0.4)	2.5 (1.9)	35.9 (4.1)
WF-APP	48.6 (1.9)	8.01 (0.4)	20.1 (1.0)	93.5 (0.4)	0.24 (0.06)	1.0 (0.1)	49.4 (1.9)

TGA/DSC results and discussion

Baseline WF-60. The TGA/DSC results for the reference WPC (WF-60) are discussed first, including the effects of weathering, to provide a baseline understanding of the results for the presence of air versus N_2 and of the FRT WPCs discussed in the next paragraphs. The TGA results for the baseline WPC are provided in Figure 1. The pyrolysis of the WF and HDPE components are easily identified in the mass fraction curve as function of temperature. Wood pyrolysis, resulting in 44.2% mass loss, occurs between 100°C to 443°C[36,37,46] and has temperature regimes for mass losses of extractives, hemicellulose, cellulose, and lignin that has minimal overlaps. For example, in Figure 1, the mass loss is initially 2.5% for the temperature range of 100°C to 200°C (with a plateau at 200°C) that is attributable to the extractives after ruling out mass losses from the other components. The next temperature regime is arbitrarily 200°C–300°C, resulting in 7.5% mass loss attributable mainly to the hemicellulose degradation with minimal overlaps with cellulose and lignin degradation. The overlaps with cellulose degradation in this temperature regime are because the cellulose

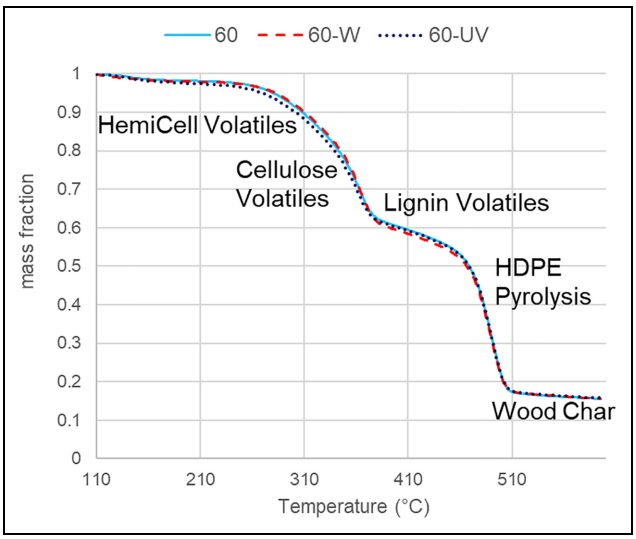

Figure 1. TGA in N_2 profiles of the untreated WPCs as unexposed, exposed to water only (-W) and exposed to UV and water (-UV) following the ASTM D2565 (ASTM 2008) accelerated weathering.

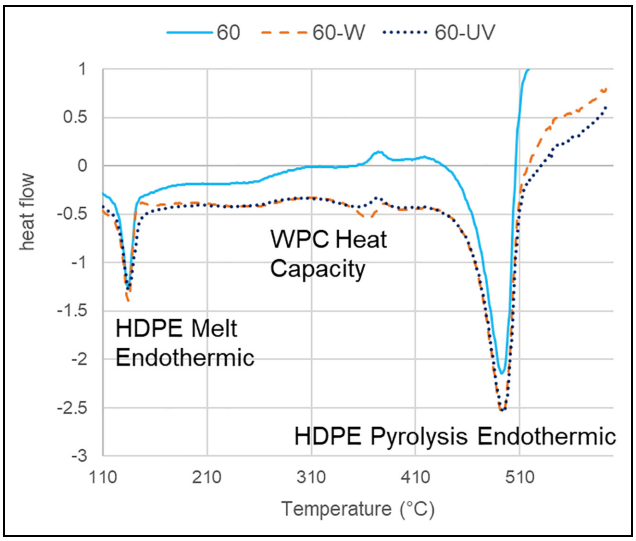

Figure 2. DSC in N_2 profiles of the untreated WPCs as unexposed, exposed to water only (-W) and exposed to UV and water (-UV) following the ASTM D2565 (ASTM 2008) accelerated weathering.

degrades quite slowly via mainly dehydration in a slight exothermic condensing carbon-linking that forms the char and water vapor.[47] However, hemicellulose degradation with minimal charring is suspected to be endothermic[48] such that the overall heat of pyrolysis for wood could be negligible in this regime.[36,37] The introduction of effective FR, particularly salt based, accelerates this charring process,[36,37] so that less of the virgin cellulose is available for breakdown to tars without attendant charring beginning at around 300°C.[47] The next temperature regime is 300°C–370°C for 25.3% mass loss in which it is known that cellulose is decomposing rapidly, probably into tars, and leaving minimal char. Finally, the temperature regime of 370°C–443°C resulting in 8.9% mass loss is attributed mainly to lignin pyrolyzing gases and leaving considerable char. According to Tang and Eickner[36], Rowell and Dietenberger,[37] the presence of FR has negligible effects on the lignin degradation. The PE and lubricating oil completely pyrolyze into gases[38] to provide the remaining mass loss of 40% in the temperature regime 443°C–595°C, leaving the wood char mass of 15.8% of the initial WPC weight that is mostly lignin residue. These mass losses in terms of percentage of the initial wood mass are: 4.2% for extractives, 12.5% for hemicellulose, 42.4% for cellulose, and 14.8% for lignin, leaving char as 26.3% of initial wood mass, which are reasonable values for a typical wood material.[36,37,46] We note that the weathering had minimal effects on the thermal degradation processes as shown by the three curves being collated together in Figure 1, whether exposed to water alone or to a combination of UV and water. It is seen that replicate tests were then not necessary.

The pyrolyzing PE and lubricating oil produce the high heat of pyrolysis, high heat of combustion (that of C_2H_4 production[38]), and MLR as shown in Figures 2 and 3. The results from the DSC in Figure 2 shows negative peaks, the first at around 135°C attributable to PE melting and the second at around 490°C attributable to PE pyrolyzing mostly the C_2H_4 gas. Note that there is no discernable heat of reaction with pyrolysis for wood material in

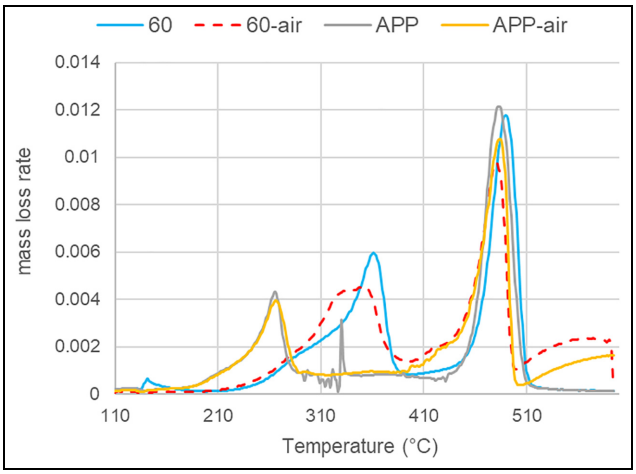

Figure 3. Effect of N_2 and air on the DTG profiles for unweathered WF-60 and WF-APP-WPCs.

the intervening temperatures, which contradict assumptions of some wood pyrolysis CFD modeling based on the Stefan-type processes, although it is conceivable the melted HDPE on the char structure will instead be responsible for Stefan-type processes, as we will show later with char modeling.

The differentiation of the WF-60 TGA results with time (DTG) is shown in Figure 3. As confirming the previous discussion, the shoulder in the temperature range of 200°C to 300°C is attributed to pyrolysis of the hemicellulose. The DTG peak at 365°C is primarily due to cellulosic volatile production and some attendant charring, and the peak at 490°C is due to the HDPE that does not char, and finally because of being in nitrogen gas the lignin mainly chars. From Figure 3, the presence of air (1) shifts the cellulose pyrolysis peak at 365°C to slightly lower temperature and broadened, (2) promotes charring oxidation of the cellulose component at temperatures above 400°C, (evident also with a small positive DSC, not shown), (3) after the HDPE completes its pyrolysis that had pushed aside the air (and not itself being oxidized), the wood char oxidizes rapidly (dashed red curve), and (4) even flaming of simple combustible gases at temperatures above 510°C that resulted in the very large positive DSC values (not shown). We note that all the FRT WPCs tested were able to suppress the glowing combustion significantly at high temperatures to achieve low char oxidation rate. An example is the solid yellow curve above 500°C for the WF-APP-WPC being considerably less than of WF-60 WPC represented by the dashed red curve. This means once the external heat source is removed, the glowing treated material will likely self-extinguish via the convective heat losses as overwhelming the heat gain from the smoldering combustion. For WF-APP, the presence of air did not affect the wood pyrolysis peak at ~260°C but did affect the wood char surface oxidation occurring immediately before and after the HDPE pyrolysis.

FRT effects at low temperature. One significant reduction in flammability can be achieved by reducing the HRR. Figures 4–9 use evidence from TGA and DSC showing that the differing FRTs have different effect on the thermal degradation process in the important lower

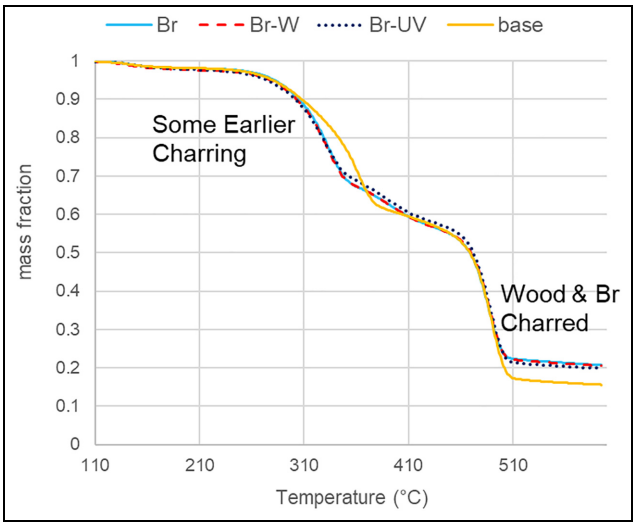

Figure 4. TGA profiles of the bromated WPCs as unexposed, exposed to water only (W) and exposed to UV and water following the ASTM D2565 (ASTM 2008) accelerated weathering.

temperature regimes that represent flaming conditions. Since the heat of combustion for HDPE volatiles is high and difficult to modify, the easier approach is to attempt to lower the volatile production rates by various mechanisms, which has been successful in the case of wood, particularly with BR, or MH, or APP additives at relatively low concentrations.

In the case of WF-BR, there is barely any effect in comparison to WF-60, including weathering, in the TGA profiles of Figure 4 and the DSC profiles of Figure 5. The only beneficial effect is the slight effect of an earlier charring of the wood component and a slightly higher char in the end in comparison to the baseline.

In the case of WF-MH, the main effect is the simultaneous increase in cellulose charring and production of MH degradation into MgO that is the equivalent of ~20% reduction in baseline wood volatiles, including a small dilution with water vapor from the degradation. No decrease in the HDPE volatiles as compared to the baseline could be discerned with the MH additive as shown in Figure 6 in the temperature regime 443°C to 595°C. In the temperature regime 370°C to 443°C, the MH TGA curves are parallel to the yellow TGA base curve, meaning that no effects on the lignin degradation could be discerned either. The Mg(OH)2 started to emit water vapor and convert to the insulating residue MgO from about 270°C[49] in an endothermic decomposition as shown in the DSC profile up to 450°C in Figure 7. This means that any imposed heating is further being absorbed by MH, thus further retarding the rise in the WPC temperature in the product end use. Whereas the TGA constrains the temperature rise rate via source heating controls that would tend to obscure this process. The retarding of the temperature rise rate helps prevent the cellulose component from rapidly obtaining the temperature regime of ablating various tar compounds above 300°C and thereby having longer duration in the continuous and slower condensation reactions of charring. Since the literature lacks information on feasible chemical mechanisms promoting the wood charring by the MH additive, we offer the above explanation for the increased cellulose charring evident in Figure 6, and which accelerated weathering has no apparent effect on the WPC degradation in the TGA testing environment.

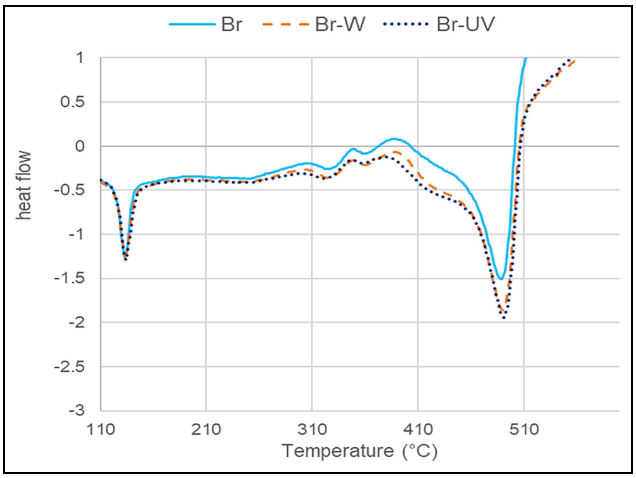

Figure 5. DSC profiles of the bromated WPCs as unexposed, exposed to water only (W) and exposed to UV and water following the ASTM D2565 (ASTM 2008) accelerated weathering.

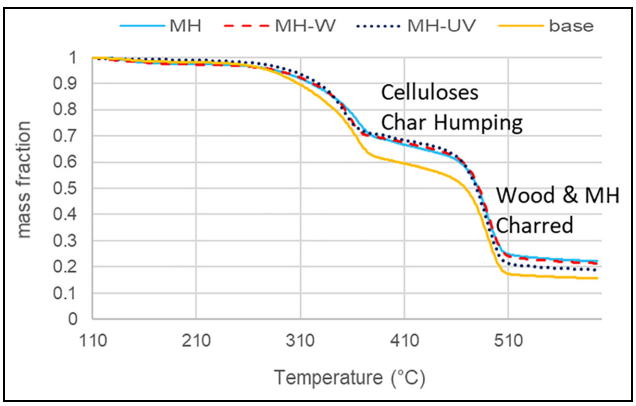

Figure 6. TGA N2 profiles of the WF-MH WPCs as unexposed, exposed to water only (W) and exposed to UV and water following the ASTM D2565 (ASTM 2008) accelerated weathering.

In the case of APP, it is obvious that APP affects both the wood and PE degradation as shown in Figure 8. Early charring at 275°C and slightly more char mass (about 5% of original WPC mass) of both hemicellulose and cellulose, is being chemically induced by the APP to further the dehydration process with condensation reactions, as confirmed also by the DSC slightly exothermic peaks around 275°C in Figure 9.[36,37] However, no enhancement to the lignin charring[36,37] is indicated in Figure 8 as the solid blue line of WF-APP being parallel to the yellow solid line of WF-60 in the temperature range 370°C–450°C, confirming. However, significant development of the HDPE charring is occurring (about 14% of WPC mass, almost as much as the wood charring) starting at temperatures greater than 443°C. The DSC results in Figure 9 has the HDPE endothermic peaks lessened from that of the base WPC because of reduced virgin HDPE available for ethylene production. The literature

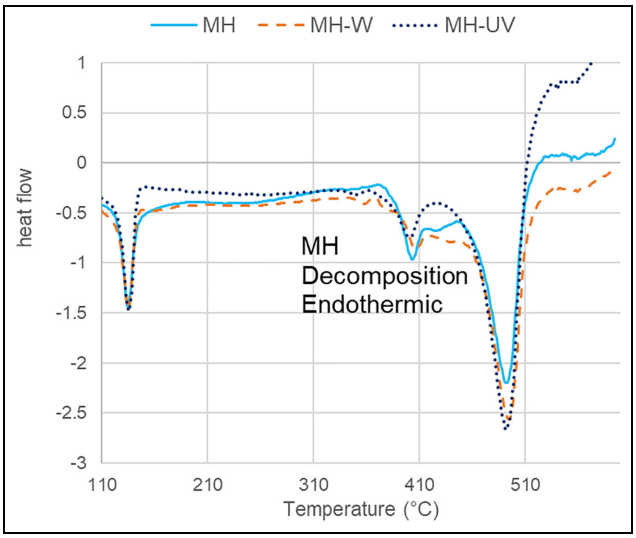

Figure 7. DSC profiles of the WF-MH WPCs as unexposed, exposed to water only (W) and exposed to UV and water following the ASTM D2565 (ASTM 2008) accelerated weathering.

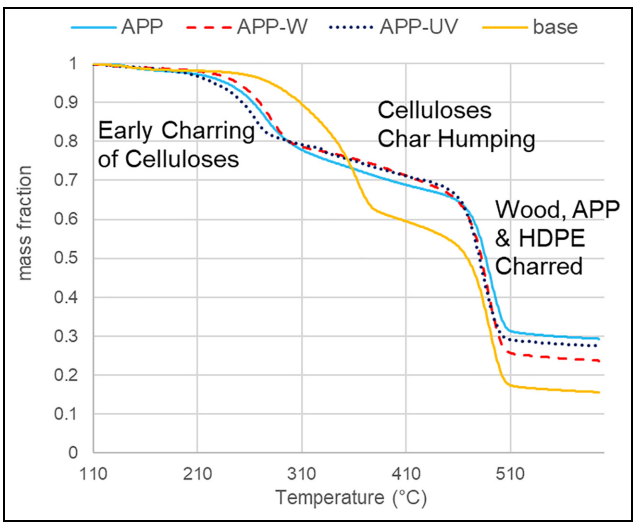

Figure 8. TGA profiles of the WF-APP-WPCs as unexposed, exposed to water only (W) and exposed to UV and water following the ASTM D2565 (ASTM 2008) accelerated weathering.

on mechanistic pyrolysis modeling[38] indicates the introduction of the dehydration and intumescent process to the HDPE induced by the APP locally present for reducing the PE MLR (blue solid line) that is evident in Figure 3 for temperatures greater than 443°C. On the contrary, the wood charring enhanced by APP has an added advantage of volatile dilution by water vapor production during charring that lowers the flaming heat of combustion, a feature also shared by the MH.

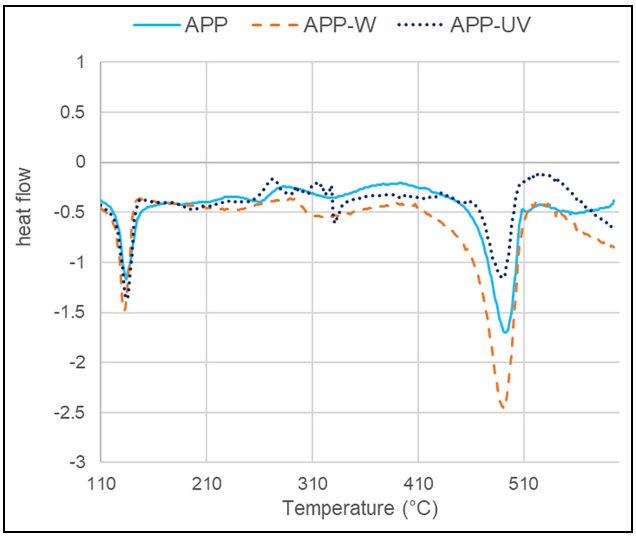

Figure 9. DSC profiles of the WF-APP-WPCs as unexposed, exposed to water only (W) and exposed to UV and water following the ASTM D2565 (ASTM 2008) accelerated weathering.

The high char development evident in Figure 8 for WF-APP-WPC in comparison with the other WPCs might lead to asserting that treatment with APP will give the best fire performance. However, MH has superior physical properties of high heat capacity, heat of reaction during pyrolysis, and relative residual weight, all of which translates to retarding the temperature rise rate in the end-product, thus possibly giving a greater char development than is immediately evident in a TGA test environment.

Fire performance tests—cone calorimeter HRR profiles explained

Representative HRR versus time curves for weathered WPCs with and without FRs are shown in Figure 10 from the cone calorimetry tests of thermally thick WPC material. We provide a detailed explanation informed by TGA/DSC results above and modeled material surface temperature profiles described below. Overall, the APP decreased the HRR the most, but also led to a smaller HRR for a longer duration, as surmised from its high charring behavior discussed earlier, in which the HDPE and wood are both charring.

The peak HRR for these FRT samples tended to follow differently than what we had observed earlier for the un-weathered samples[21] which we will explain in the next section on the weathering effects on the HRR. The greater emphasis will be on the overall HRR profile and how that relates to the flammability of these WPCs.

It should be noted the TGA/DSC tests were done with thermally thin samples, so that the thermal conductivity is removed as a variable in those tests. However, the demonstration of charring for all WPCs with the TGA/DSC tests, implies that a heating thermal profile (that includes thermal conductivity) propagates through the thick charring material when exposed to irradiance in the cone calorimeter tests. Visible degradation at fixed temperatures, which is around 300°C for untreated wood and around 475°C for HDPE, will mean the thin

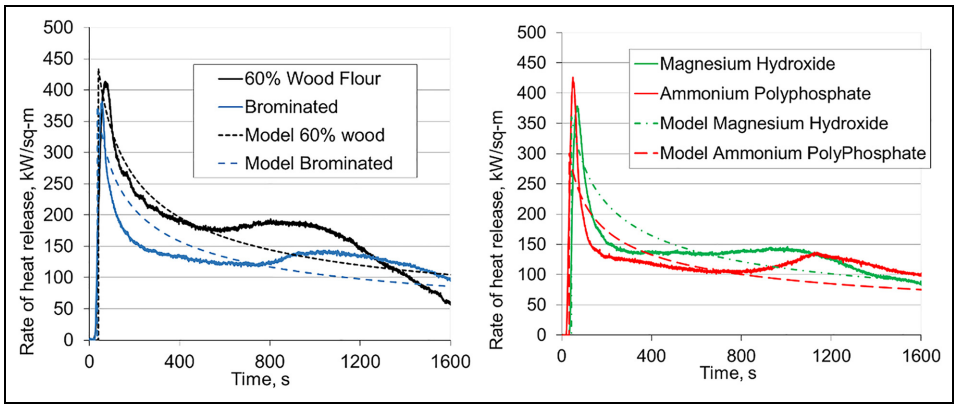

Figure 10. HRR profile during charring for the WPC samples, with model predictions.

degradation layers at those two temperatures are moving inward in the material at a decreasing char rate that is proportional to the charring material MLR, and also to the flaming HRR providing that the heat of combustion is relatively constant (around 24 kJ g^{-1} for up to 1000 s for the WPCs in the cone tests) and the local char mass is also relatively constant during charring as discussed by Lyons.[28] That is, an approximate equation for the HRR and MLR during flaming based on pyrolysis fronts (i.e., mean positions of narrow pyrolysis zones for component materials) is

$$\mathrm{HRR} = h_{c,,w} f_{v.w} \rho_m v_w + h_{c,p} f_{v.p} \rho_m v_p + h_{c,a} f_{v.a} \rho_m v_a \tag{2}$$

$$\mathrm{MLR} = f_{v.w} \rho_m v_w + f_{v.p} \rho_m v_p + f_{v.a} \rho_m v_a \tag{3}$$

So that in addition to the wood charring front rate, v_w, we also have the melt (i.e., HDPE and lubricant liquid) pyrolysis front rate, v_p, and the FRT additive pyrolysis front rate, v_a, with each component contributing their share of volatile mass fraction, $f_{v,i}$, of the composite density, ρ_m, and volatile EHOC, $h_{c,i}$ (kJ g^{-1}), that release the heat in the flame above the sample. Overall, this leaves behind the charred mass fraction, $f_{char} = 1 - (f_{v.w} + f_{v.p} + f_{v.a})$, for possible surface oxidation with air once the flames became erratic and diminished (afterglow). The overall volatile EHOC is the HRR divided by the overall volatile mass flow rate, MLR. Focusing on one of the tests with the WF-60 as a base WPC, that does not include the FRT additive, we can simplify equations (2) and (3) somewhat by assuming a composite pyrolysis front rate as an average as, $v_m = 0.5 * (v_w + v_p)$, to insert in place of the individual rates in equations (2) and (3), and invert the equations to solve the composite pyrolysis front rate as function of either MLR or HRR, and numerically integrate with time. The results are shown in Figure 11 by utilizing the volatile fractions, $f_{v.w} = 0.482$ and $f_{v.p} = 0.4$ (agreeing with the measured residue fraction of 0.118) and providing the ending composite char depth as shown by the blue dashed curve, via equation (3) of 13.5 mm. However, the more severe comparison is using the measured EHOC of wood as 13 kJ g^{-1} (separate cone calorimeter test for solid pine) and EHOC of HDPE/lubricant as 38 kJ g^{-1} (near the end of test and after the wood is fully charred), we obtained the orange dotted curve via equation (2) (for HRR estimation), that is at most 7.8% less than the blue dashed curve at the quarter-way

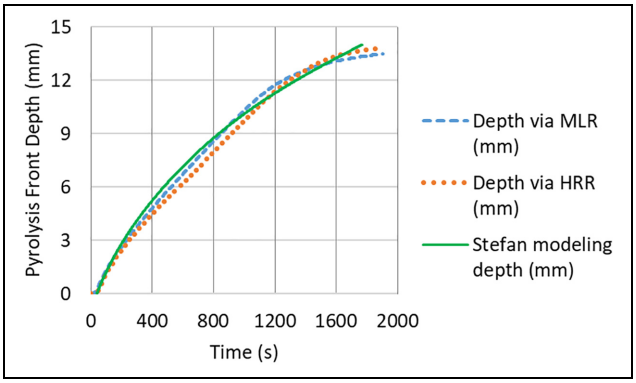

Figure 11. Derived composite char depth as function of time using averaged char front rates in place of specific pyrolysis front rates in equations (2) and (3) and comparison with Stefan process modeling from equation (9) (with equations (7) and (8)).

point. Thus, taking equation (2) divided by equation (3) using the composite pyrolysis front rate in place of the individual pyrolysis front rate we obtain the predicted composite EHOC = 24.3 kJ g^{-1}, in relatively good agreement with the cone calorimeter value of EHOC = 24.9 kJ g^{-1} for Test D. The fitted parameters are listed in Table 3.

As for the WPC with FRT, the determination of volatile fractions of the components can be assisted with results from the TGA and DSC tests, and the known behavior of the melt and FRT components. According to TGA results, only the APP can reduce the volatile mass fraction of the melt (PE and lubricant) to a measured estimated value of 0.29, whereas it remains at 0.4 for the BR and MH additives that has nil effect on the melt. From the literature, the BR FRT will volatize,[50] with a volatile fraction of 0.06. However, MH volatizes water vapor, leaving behind MgO,[51] for the volatile fraction (on basis of WPC mass) of 0.031, and APP volatizes mainly ammonia and water vapor, ultimately leaving behind P_2O_5[52] for a volatile fraction of 0.027 of WPC mass. Since we terminate the cone calorimeter tests at flameout and avoid the afterglow, the char mass fraction is measured (last column in Table 3), so then the volatile mass fractions for the wood component are obtained from the mass balance. Given that the wood's final char value is known to be affected by the temperature profiles, the residue weight measured in the cone calorimeter test is expected to vary somewhat from the TGA tests that involve quite low heating rates. As to their EHOC values of the volatiles for the FRT affected components, they were fitted to the cone calorimeter data, given how well the independent measures for the wood and melt EHOC predicted well the composite pyrolysis front rates determined with equations (2) and (3) as shown in Figure 11. Later we discuss how this leads to determination for the total heat of gasification with Stefan process modeling.[28]

As to the slab being intact and perhaps intumescent during charring, Figure 12 shows the WF-APP-WPC clearly performing better than the other WPC formulations. In the picture we see that the char remains from the cone calorimeter tests show the APP FR additive induces a nice black and relatively intact char shown on the far right side of the picture. The untreated WPC char on the left seems like it is crumbling apart, while the two slabs in the middle for the other FRT WPCs are seemingly intact.

Table 3. Charring parameters of WPCs derived for equations (2) and (3)

Code	$f_{v.w}$	$f_{v.p}$	$f_{v.a}$	$h_{c.w}$, kJg^{-1}	$h_{c.p}$, kJg^{-1}	$h_{c,a}$, kJg^{-1}	f_{char}
WF-60	0.482	0.4	0.0	13	38	0	0.118
WF-BR	0.350	0.4	0.06	13	29	0	0.190
WF-MH	0.349	0.4	0.031	11	38	0	0.220
WF-APP	0.350	0.29	0.027	10	38	12.3	0.333

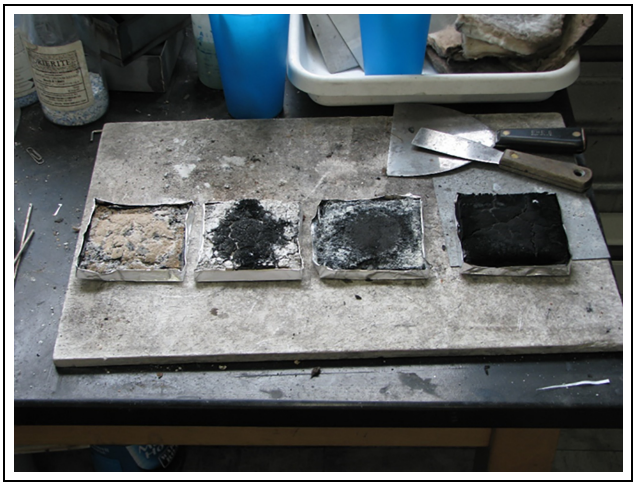

Figure 12. Charred WPC slabs from left to right, are WF-60, WF-MH, WF-BR, and WF-APP.

To understand the HRR profiles more fully and justify equations (2) and (3) in its use of the pyrolysis front rates, we include representative surface temperature measurements of the irradiated side and the unexposed side of the WPC for WF-60 as shown in Figure 13. Three distinct regions of thermal behavior can be discerned. From 0 to 50 s is the classical heat response of the thermally thick material.[28] The ignition of WPC occurs within 20–30 s (Figure 10 using HRR = 24 kW m^{-2} criteria). Indeed, using the thermal properties in Table 4 and an accurate prediction for surface temperature of finitely thick materials[53] shown in Figure 13 as the green solid circle points, which at the IT of 28 s predicts surface temperature at ignition of 367°C. This is typical of the wood materials and is much less than the pyrolysis temperature of the HDPE at around 485°C. Although the surface thermocouple has already detached right after ignition (>28 s) as shown as the orange filled triangle point in Figure 13, it is likely that by the time of PHRR for all WPCs, the HDPE component is pyrolyzing in its thin pyrolysis zone (or front) within the wood char instead of remaining on the surface (as would be for pure plastic), especially given the EHOC is ~24 kJ g^{-1} at the PHRR. Turning our attention to the back surface temperature data, as shown by the dashed black line, there is the question as to the time duration in which all three pyrolysis fronts are moving in tandem in this second region of thermal behavior. The key to this determination is to address the evident two-phase Stefan problem, as for example occurs in the

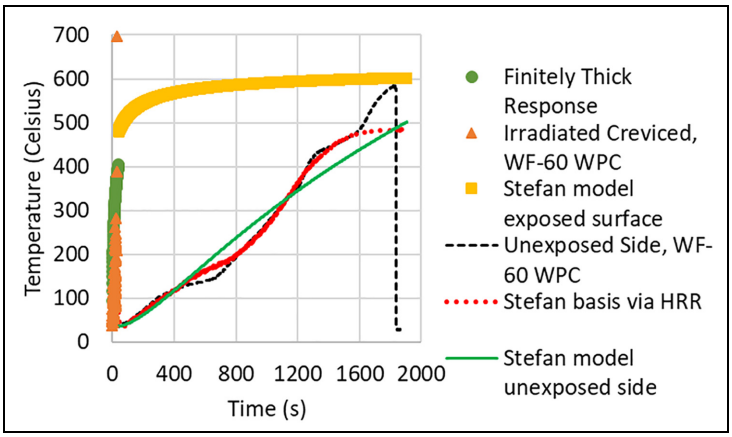

Figure 13. Surface temperatures of WPC slabs exposed to 50 kW m^{-2} irradiance.

Table 4. Thermal parameters of WPCs components for ignition/Stefan process modeling

Code	ρ, gm^{-3}	t_{ig}, s	t_h, s	C_p, JK^{-1} g^{-1}	k_o, Wk^{-1} m^{-1}	h_v, J g^{-1}	T_{ig}(calc), K
Pine wood	–	–	–	2	0.15	0	–
HDPE & Lub	–	–	–	1.6	0.33	1800	–
BR	–	–	–	2	0.15	−2000	–
MH	–	–	–	1.33	0.5	1356	–
APP	–	–	–	2	0.15	0	–
WF-60 WPC	967,111	28.0	40	1.84	0.222	720	641
WF-60 Char	114,370	–	–	15	0.0263	–	–
WF-BR WPC	1,000,222	26.4	36	1.84	0.222	520	632
WF-BR Char	190,198	–	–	15	0.0422	–	–
WF-MH WPC	962,640	33.9	44	1.77	0.257	855.6	649
WF-MH Char	212,320	–	–	15	0.0567	–	–
WF-APP-WPC	1,044,963	19.8	34	1.84	0.222	720	598
WF-APP Char	348,469	–	–	15	0.074	–	–

freezing of surface water on a lake. It is known that when cellulose undergoes charring via dehydration process accompany by carbon condensing reaction (primarily in the range 200°C–300°C), the reaction is exothermic.[36,47] However, our DSC result in Figure 2 indicates no peaks (i.e., nil heat of reaction for pyrolysis) for the wood component, meaning that the pyrolysis of the hemicellulose and extractives evidently involve an endothermic reaction process[48] canceling the charring heat from the cellulose, at least for the pine species that we used. Above 300°C, the cellulose degrades via an endothermic fragmentation into volatile anhydrosugar,[47] whereas the lignin is charring exothermally[48] to perhaps match the required heat for the cellulose fragmentation. However, the significant endothermic heat of reaction for HDPE pyrolysis ($h_e = 1800$ J g^{-1}) may permit a simplified Stefan analysis as follows.

Unchanging thermal parameters are: $\delta = 3.5$ mm, $T_o = 33.3$°C, $T_e = 480$°C, $\epsilon = \alpha = 0.97$, $k_r = 9.5$ E−10 Wm^{-1} k^{-4}, and $h_{conv} = 21$ WK^{-1} m^{-2} at $q_{cone} = 50$ kW m^{-2}.

Assuming a quasi-steady state composite material pyrolysis front rate, v_m, the thick bulk material attains a steady temperature profile as a solution to the simple Stefan problem as applied to pure plastics and extended here to the WPC[28] as

$$(T - T_o) = (T_e - T_o) exp\left(\frac{-v_m\, y}{\left(k_c/\rho_m C_{p,m}\right)}\right) \tag{4}$$

Where the variable y is the distance into the bulk material away from the evaporation front. The heat can continue to flow from the back surface into the sample holder in a steady fashion, with form of equation (4) maintained if the thermal diffusivity stays constant, despite the low thermal conductivity of the insulating back material. The back surface temperature can be predicted from equation (4) by using the composite pyrolysis front rate from equation (3) and replace the variable y by the expression, $\delta - \int_{t_h}^{t} v_m dt$, so that the profile temperature T is replaced by the back temperature, T_b. Note that the depth of the composition pyrolysis front is shown in Figure 11 as the dotted filled orange points. The beginning time of char growth t_h correspond to the HRR that is approximately one-half of the PHRR, and still greater than the ignition criteria of HRR = 24 kW m^{-2}. Thus, when the composition pyrolysis front depth reaches the material thickness, δ, the back surface temperature is predicted to be the composition pyrolysis temperature, T_e. By fitting equation (4) to the back surface temperature data, we obtained the red dotted line in Figure 13 as an excellent fit, and a composition pyrolysis temperature of 480°C, which corresponds to the HDPE as determined by DSC in Figure 2, and other reasonable thermal properties listed in Table 4. The simple Stefan condition therefore covers the time shortly after ignition to 1600 s and is adaptable to a changing net surface heat flux but still at greater than the imposed irradiance of 17.2 kW m^{-2}. The consequence for validating equation (4) is a constant value for the total heat of gasification per unit original mass WPC[28] at the PE pyrolysis front, h_g, used in the gasification heat flux expression,

$$q_g = v_m \rho_m \left(f_w h_w + f_e h_e + f_a h_a + C_{p,m}(T_e - T_o)\right) = v_m \rho_m h_g \tag{5}$$

Thus, the Stefan phase change problem has been simplified to determining the heat flux from the char into the PE pyrolysis front so that equation (5) for the gasification heat flux can be used to determine the composite pyrolysis front rate, and therefore in turn be used in equation (2) to predict HRR and in equation (3) to predict the MLR. To simplify the heat balance within the char layer itself, we would realize the portion of cone's irradiant flux being conducted into the char layer is (1) adjusted by the flame and surface condition by using the absorptivity parameter, (2) reduced by char surface thermal radiation into the environment, (3) reduced by heat absorption in char heat capacity, and (4) reduced by heat absorption in the outgassing volatiles, in order to result in the conducted heat flux needed for the gasification heat flux given by equation (5). As part of simplification, we note the heat absorption by char heat capacity and outgassing volatiles are assumed small compared to cone's irradiance and radiant heat losses from the char surface. This results in the char heat balance being modeled as follows. Beginning with the thermal diffusion equation of a moving solid material,

$$\frac{1}{\rho_{ch}C_{p,ch}}\frac{\partial}{\partial x}\frac{k_{ch}\partial T}{\partial x}=\frac{\partial T}{\partial t}+v\frac{\partial T}{\partial x}\approx\left(\frac{x}{\delta_{ch}}\right)\frac{\partial T_s}{\partial t}+v_m\left(1-\frac{x}{\delta_{ch}}\right)\frac{\partial T_{ch}}{\partial x} \tag{6}$$

where the coordinate system is fixated to the composite pyrolysis front with the variable x is positive toward the char layer from the pyrolysis front (i.e., $x=-y$). We note that the exposed surface temperature, T_s, changes rapidly with time immediately after ignition, but the temperature at the pyrolysis front remains fixed at 480°C, and the rate of local temperature change is modeled approximately linear with x to avoid the complicated rigorous solution to the two-phase Stefan problem. Likewise, the movement of pyrolyzing PE material into the char layer will experience a temperature rise rate from that movement and will diminish at the char surface as the char temperature gradient get small, which we again approximate as decreasing linear variation with x to avoid the rigorous solution. Integrating equation (6) with respect to the variable x and using the heat flux relation, $q=-k_{ch}\partial T/\partial x$, at the boundaries we derived the heat balance equation used for solving ultimately the needed gasification heat flux

$$\frac{1}{\rho_{ch}C_{p,ch}}\left(\alpha q_{cone}-\varepsilon\sigma\left(T_s^4-T_o^4\right)-q_g\right)=\frac{\delta_{ch}}{2}\frac{\partial T_s}{\partial t}+v_m\frac{\delta_{ch}}{2}\frac{q_g}{k_{ch}} \tag{7}$$

While utilizing equation (5) to relate the composite pyrolysis rate v_m to the gasification heat flux q_g and substitute into equation (7). To make further progress, we double integrate equation (6) with respect to the variable x to solve for the exposed surface temperature, T_s, with the result

$$\int_{T_e}^{T_s}k_{ch}dT=q_g\delta_{ch}+\rho_{ch}C_{p,ch}\left(\frac{\delta_{ch}^2}{6}\frac{\partial T_s}{\partial t}+v_m\frac{\delta_{ch}^2}{3}\frac{q_g}{k_{ch,}}\right) \tag{8}$$

where the char thermal conductivity is modeled as the expression $k_{ch}=k_o+k_rT^3$, that includes the radiant heat exchange between the char particles which is proportional to temperature to the third power. The explicit numerical integration of the surface temperature rate involved a division by zero, so it meant solving equation (8) implicitly instead for the surface temperature T_s and in conjunction with equation (7), will involve a matrix equation to solve for both T_s and q_g, and solving for the composite char depth from the integration of the composite pyrolysis rate as (Euler numerical integration was adequate),

$$\delta_{ch}=\int_{t_h}^{t}\frac{q_g}{\rho_m h_g}. \tag{9}$$

The green solid curve in Figure 11 represents this char depth solution for base WPC, along with the solution for the surface temperature shown as the yellow filled square points in Figure 13. The corresponding prediction of the unexposed surface temperature (using equation (4)) is shown as the green solid curve in Figure 13 in relatively good agreement with the data given by the black dashed line. The prediction of HRR from equation (2) using the Stefan solution for the composite charring rate is shown in Figure 10 as the black dotted line in comparison to the measured HRR with the solid black line. A good prediction of the data is obtained up to 600 s. Since the HOC remains around 24 kJ g^{-1} from 600 to 1200 s,

indicating the anerobic condition as remaining within the char, we postulate shrinking of the char (as observed in Dietenberger[46] with 10% linear shrinkage of thin charring wood) that give rise to higher char thermal conductivity and lowered char thickness that then give rise to an increased gasification heat flux, to explain the higher HRR than expected at greater than 600 s. The shrinking of the char seems evident in the charred samples in Figure 12 as the exposed surface is quite below the aluminum foil wrapping edge for the WF-60 sample, whereas no char shrinkage is evident for the black WF-APP sample. At 1240 s, upon the back surface reaching 380°C, the wood component should cease its pyrolysis and therefore terminating its pyrolysis front. Thus, the second region is from 50 to 1240 s due to the existence of both wood and HDPE pyrolysis fronts implied in equations (2) and (3) and confirmed in Figure 13. Finally, the third region is from 1240 s to the test end, where the HDPE is only volatizing, with its EHOC observed to increase and approaching 38 kJ g^{-1} or higher, corresponding to pure PE.

Various strategies for reducing the HRR become evident when using the FRT additives. Since we are retaining 35% HDPE as a practical WPC material fraction, the options for improving the PHRR (by decreasing it) that coincides with the nearly zero composite char thickness, are limited to increasing the heat of gasification, decreasing the combustible volatile fraction, and decreasing the volatile heat of combustion. During charring, a thicker char layer at higher char density to reduce the gasification heat flux q_g for reducing the bulk HRR (i.e., using the HRR at 600 s) could be a worthy goal, but to get quickly to the thicker char layer will require a high initial char rate that will also increase the PHRR somewhat. To better sort the various mechanisms for reducing HRR, we used the charring model to identify the importance of adjusting the thermal parameters. A sensitivity analysis that this would imply will not be necessary for this study, given the various mechanisms inherent in the selected FRT as BR, MH, or APP at the 10% additive level.

At 600 s the WF-60 has a predicted HRR of 164 kW m^{-2} and a predicted PHRR of 434 kW m^{-2} indicating that the charring model seems adequate in predicting a decreasing HRR with time as shown in Figure 10. The parameters in Tables 3 and 4 were adjusted reasonably to obtain the model predictions shown in Figure 10 in fitting the data for that shows WF-BR and WF-MH equally decreasing base HRR of WF-60 by around 17% and the WF-APP has the most decrease of base HRR of WF-60 by 31%. More specifically, the BR decreases the PE EHOC to 29 J g^{-1} that resulted in decreasing HRR by 17%, but there is 6% increase in HRR due to exothermic charring (i.e., net reduction in heat of gasification that is also implied in the DSC results for BR) that is compensated by 8% decrease in HRR from the dilution effect of BR pyrolyzing. In the case of MH, there are small multiple reductions in the resulting HRR, such as 4% HRR reduction due to increasing h_g, a 5% HRR reduction due to dilution of PE and WF volatiles, a 4% reduction in HRR due to reduction in WF volatile fraction, and 3% reduction in HRR due to decreasing the WF EHOC to 11 kJ g^{-1}. Finally, the WF-APP achieves the most HRR reduction as follows, (1) reducing the HRR by 21% primarily from reducing the PE volatile fraction to 0.29 from 0.4, (2) further reducing the HRR by 4.5% due to reduction in the WF volatile fraction to 0.35, (3) further reducing the HRR by 4.9% due to reduction in WF EHOC to 10 kJ g^{-1}, and (4) further reducing HRR by 0.6% due to dilution effect (note that APP has EHOC of 12.3 kJ g^{-1}). If the strategy of best improving the fire performance can be summarized, it would be that the already good charring behavior of the base WPC is improved by increasing the char fractions, first of the PE component and then of the WF component, while not compromising much on the heat of gasification, on the dilution of combustible volatiles,

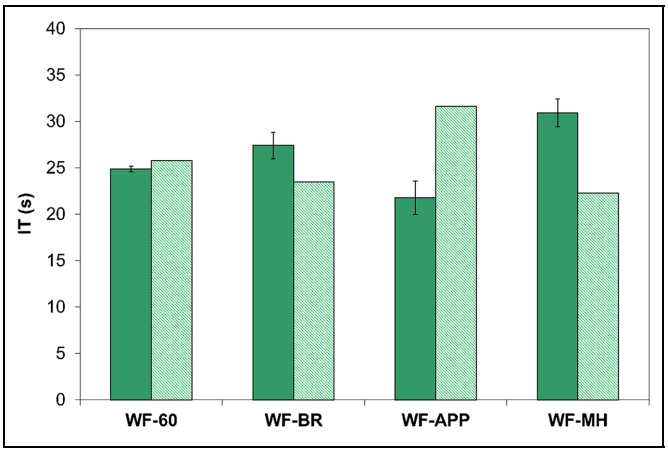

Figure 14. Ignition time for four WPCs: dark green is before, and light green is after weathering.

and on the time to ignition. Although the MH FR mainly works by improving these latter three parameters, it only does enough in reducing HRR to at least replace the BR FR that has environmental issues.

Fire performance tests—cone summary for weathered effects

Next, we discuss the cone calorimetry results of IT, averaged MLR, and EHOC for the four WPCs showing the effects of weathering. The weathering does not change the time to sustained ignition (IT) of 25 s for the untreated WPC samples, as indicated by the WF-60 bars in Figure 14. The Bromide FR can increase the IT slightly by how it affects the combustion process (dark green WF-BR bar), but its surface leaching negates that to reduce the IT (light green WF-BR bar). The APP FR will decrease the IT slightly from the early charring, but surface leaching and/or UV modification will negate that by increasing the IT. Finally, MH FR will increase the IT slightly via densification and corresponding increase in heat capacity, but its surface leaching negates that feature by reducing the IT. Incorporating FRs in WPCs had a mixed effect on IT (Figure 14). In summary, FRs that significantly improved IT compared with WF-60 (i.e. increased it) include BR and MH, while MH increased IT by 24% and APP decreased IT by 12%, and the weathering negates the FR modification of the IT. These evident surface leaching effects were not apparent in the TGA/DSC tests, presumably because the supposed leaching region is thinner than the thin sample buttons used in the TGA/DSC tests. In any case, the time to ignition, by itself, is not a significant contributor to flammability, as will be shown by a later discussion on the HRR profile.

As might be suggested by the HRR and TGA curves of the four sample types, the FRs selected will likely increase charring, leading to the overall decrease in the MLR as shown in Figure 15. The WF-APP and WF-MH are about equal in reducing the overall MLRs by about 40%, whereas the WF-BR has a lesser reduction of the MLR of around 11%, even after having been weathered. The most improvement was shown when APP was added, while adding BR improved MLR the least. Since charring involves mass losses of thin layers within

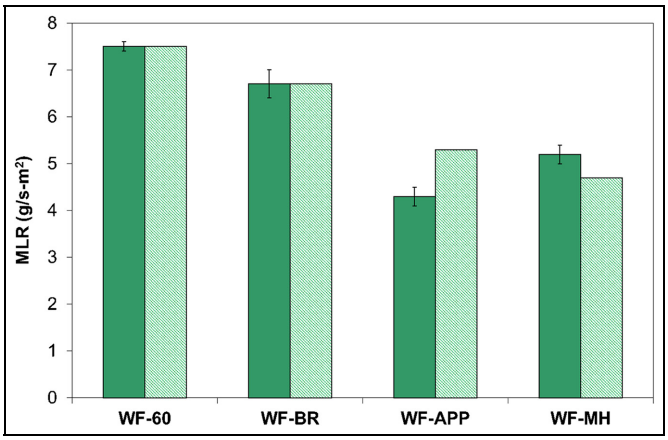

Figure 15. Mass loss rate for four WPCs: dark green is before, and light green is after weathering.

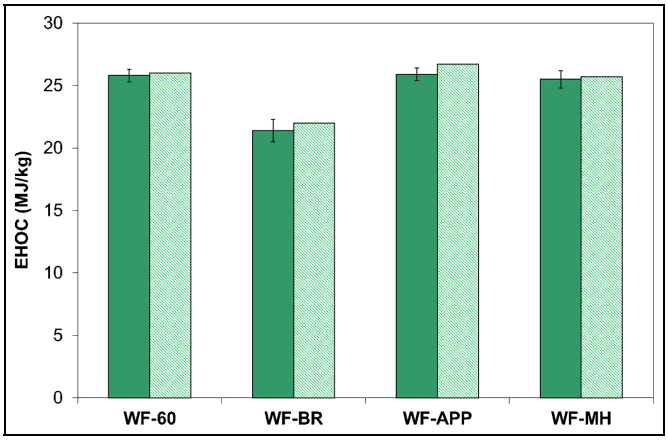

Figure 16. EHOC for 4 WPCs: dark green is before, and light green is after weathering.

the material bulk as explained earlier, we conclude there is no bulk leaching of the FRs during weathering.

EHOC in Figure 16 is the THR divided by the total mass loss, which includes both the flaming and smoldering phases, each having their own HOC. The only FR to significantly change EHOC was BR, as expected from its FR mechanism, and noting that the TGA/DSC tests do not readily address the HOC reduction. Compared with WF-60, the WPC containing BR significantly decreased EHOC by 17%. The remaining FRs did not significantly change EHOC. The reason the WF-APP and WF-MH have the similar EHOC as that of the untreated WPC, is that both their THR and overall mass loss decrease by the same amount due to the non-volatility of phosphates and magnesium. Since the BR FR had moderate decreases in both the MLR and EHOC, the overall synergistic effect on its HRR profile makes it a good FR contender for improved flammability. The weathering of the samples

had negligible effects on the EHOC (shown by the light green bars) from their un-weathered state (shown by the dark green bars), meaning that the bulk material has essentially retained the FR contents during weathering.

Fire performance tests—cone HRR detailed effects concerning weathering

Representative HRR versus time curves for weathered and un-weathered WPCs with and without FRs are shown in Figures 17–20, along with pine and Ipe as references. It is easily seen that all FRs in all conditions lower HRR of WPCs.

It is evident the weathering process had no effect on the HRR for 60-WPC in Figure 17 and BR-WPC in Figure 18, and minimal worsening effect (i.e., slightly higher HRR) on MH-WPC in Figure 19 and APP-WPC in Figure 20. Examining the un-weathered data (blue curves) versus the weathered data (orange curves), all FRs significantly improved the peak HRR and average HRRs of WPCs. Compared with WF-60, the peak HRR of WPCs decreased between 11% and 35% when FRs were added. WPCs containing MH performed the best while WPCs containing the BR performed the worst, as concerning the peak HRR. This is consistent with the total heat of gasification as listed in Table 4 for these FRs having an inverse relationship via equation (5) with the initial composite pyrolysis front rate, which is in turn proportional to the PHRR via equation (2). Indeed, the PHRR is proportional also to combustible volatile fraction and their individual EHOC, thereby complicating this analysis. Thus, the greatest weathering effect is on increasing the sharp peak HRR by as much as 30%, as it seems associated with surface leaching or UV degradation of the FRs. FRs also influenced the average HRR over the test duration. Compared with WF-60, the average HRR over the test duration decreased between 19% and 39% when FRs were added. For average HRR, APP improved the fire performance of WPCs the most. Each FR system significantly lowered the THR, ranging between 15% and 24% improvement. Although BR

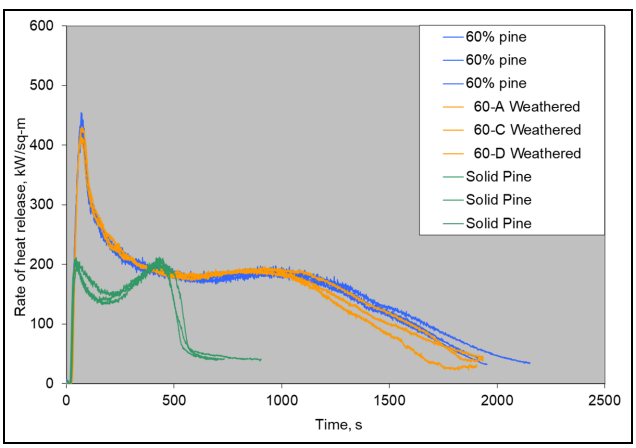

Figure 17. HRR results for weathered and unexposed 60-WPC and pine, including triplicates for each test variation. Features include a sharp first HRR peak that lessens flammability impact, a flattened second HRR peak as compared to wood, and still has higher HRR than wood, making the base WPC more flammable than wood.

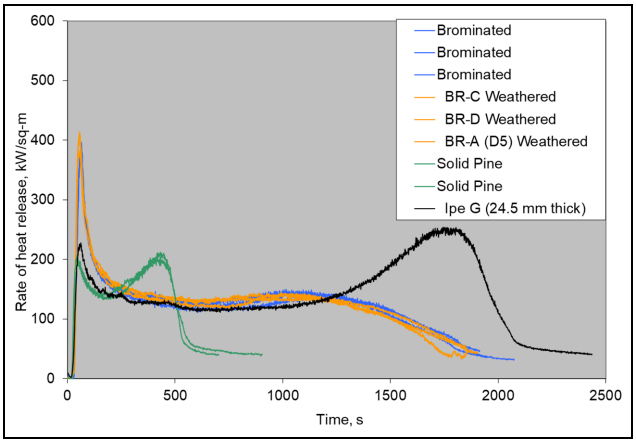

Figure 18. HRR results for weathered and unexposed BR-WPC, and pine and ipe, including triplicate tests of the WPC. Features include very repeatable tests and showing no weathering effects on BR ability to reduce the HRR, the first peak HRR appears sharper than in the case of base WPC, and still more flammable than pine or Ipe in the immediate post-peak HRR region.

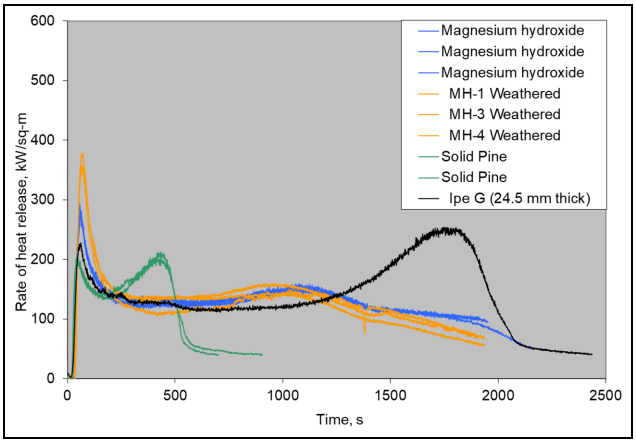

Figure 19. HRR results for weathered and unexposed MH-WPC, and pine and ipe, including triplicate tests of the WPC. Features include very repeatable tests and showing that weathering only increases the peak HRR, the first peak HRR appears sharper than in the case of base WPC, and still more flammable than Ipe in the post-peak HRR region.

improved THR the most, the performance was not statistically different from WPCs containing APP. While MH improved THR the least, the performance was not statistically different from WPCs containing APP. Otherwise, Figures 17–20 indicate that for all the FRs, we can confirm the useful synergistic role of the PE to effectively eliminate the bulk leaching of the FR.

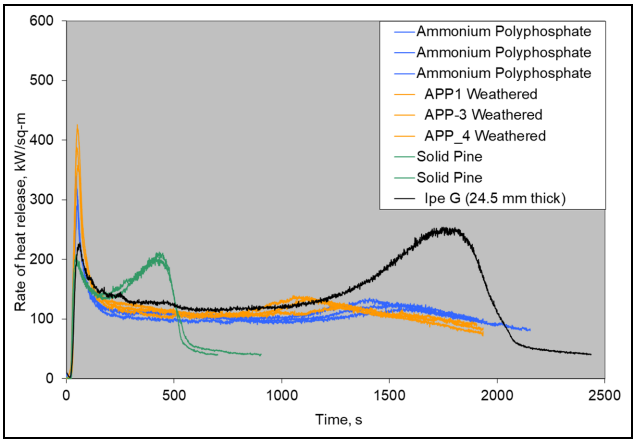

Figure 20. HRR results for weathered and unexposed APP-WPC, pine and ipe, including triplicate tests of the WPC. Features include very repeatable tests and showing that weathering only increases the peak HRR, the first peak HRR appears sharper than in the case of base WPC and is the only treated WPC less flammable than Ipe in the post-peak HRR region. The post-PHRR of the HRR plateau at 100 kW m^{-2} of up to 600 s and beyond places APP-WPC in the potential Class I FSI rating (ASTM E84).

Discussion

The development of the propensity to fire growth parameter[4,54] helps weigh the importance of lowering the HRR and THR versus increasing the time to ignition for improving flammability, particularly considering the conflicting flammability assessments within Figure 10. Variation from this observation can also occur if the heat of gasification is significant, as it would be for the PE. Indeed, the second and largest HRR peak commonly observed with wood products is associated with initiating thermally thin behavior and char combustion. A significant heat of gasification, along with the PE volatiles pushing away the incoming air at temperatures higher than that of the wood volatizing, can modify this process to eliminate the second HRR peak, as confirmed by the WPC char modeling. A warning was provided about a sharp initial PHRR that can be a misleading flammability parameter to use in some situations and that it would be better to examine the HRR behavior immediately after the initial peak[4,54] for exposure time up to 600 s, which is the test time for the regulatory ASTM E84 flame spread test[55] used in North America.

Based on the thermal Stefan process developed to explain charring, an earlier wood charring due to FRT can enhance the insulation effect for slowing the pyrolysis front rate for both WF and PE via lowering the internal heat flux needed for the gasification heat flux. Overall, APP decreased the HRR the most, but also led to a smaller HRR for a longer duration. Based on the TGA results, the APP can cause increased charring also in the PE, thus decreasing the MLR of the PE further by a chemical process, without much change in the HOC of PE volatiles. As also previously explained, the HRR profile immediately after the initial peak is the most important factor for fire growth behavior, and sooner the charring of wood is initiated, the better the outcome, as is evident in Figure 20 showing the APP giving the best result, even better than the Ipe HRR profile, with the MH and BR close behind in Figures 18 and 19. Weathering evidently has minimal worsening effects on the HRR, and

therefore the flammability, because the PE component is able to retain the FRs in the bulk region, including those FRs contained within the WF.

The following summarizes the results of this study.

- The TGA/DSC results can explain FR features concerning MLRs and heats of reactions that can be used to guide FR developments. The main WF-BR WPC effect was the slightly earlier charring, and the main WF-MH effect was increased levels of WF charring, and the WF-APP has several effects such as having earliest and the most charring of both WF and PE, thus showing the most relative potential for lowering the HRR. This possible fire performance of APP has a caveat as the other FRs have favorable physical properties not measurable with the TGA/DSC. That is, BR-based FR lowers the heat of combustion and the MH-based FR can lower MLR further with the high heat of gasification added to that of PE and increase IT due to increased heat capacity and possibly lower the EHOC through emitting diluting water vapor. All FRs had the ability to suppress the char oxidation after the HDPE had pyrolyzed.
- IT and Peak HRR measured in the cone calorimeter are affected by surface leaching and/or UV degradation of FR from the WPC. For the un-weathered WF-BR WPC, the IT was increased mildly, and peak HRR was decreased the least as the FR affected mostly the combustion processes, but when weathered, these IT and PHRR effects were negated. For the un-weathered WF-MH WPC, the IT increased the most, and the peak HRR decreased the most among the FR due to physical properties enhancement but were negated when the WPC was weathered. Finally, for the un-weathered WF-APP-WPC, the IT decreased moderately, and peak HRR decreased moderately but were negated when the WPC was weathered.
- However, the impact on fire growth behavior, as in the ASTM E84 flame spread test, has more to do with the hyperbolically decreasing portion of the HRR profile and less to the various changes in IT and PHRR. Indeed, the sharper the initial peak HRR is, with a corresponding low flat HRR profile, the more the WPC behaves similarly to a gypsum board with a thick paper coating that receives a Class I FSI. Indeed, the WF-BR WPC reduces EHOC significantly while WF-MH and WF-APP reduces MLR by about 40% in comparison to WF-60 WPC and can be related to the bulk behavior of the FR in thick samples. Overall, the improved flammability with the FRs is not affected by weathering (or non-leaching of the bulk FR) as can be determined from the post-peak HRR profile that are essentially the same between the un-weathered and weathered samples and confirmed with triplicate testing.
- In final analysis, the WF-APP-WPC is alone in providing HRR less than that of Ipe HRR in the post-initial peak HRR region and does so by primarily reducing combustible volatile fractions of WF and PE significantly as demonstrated with the Stefan-based charring model. We note (from a previous study[21]), that the best oxygen index, average HRR after 60 s, 300 s, and over the test duration, and MLR were reported when APP was used. Also, APP had a negative effect on mechanical properties. If for some reason the high initial peak HRR or low IT of WF-APP-WPC in relation to WF-60 WPC or WF-MH WPC becomes a problem (such as meeting WUI regulations discussed in the introduction), one could include the MH into the surface layer of WF-APP-WPC to further reduce the peak HRR and increase the IT.

Conclusion

There is potential for WPCs to expand into new and existing applications in the residential construction and furniture industries. However, incomplete knowledge regarding the fire performance of WPCs and the effectiveness of FRs limits this expansion. In this study, we used primarily TGA/DSC and cone calorimetry to characterize the fire performance of WF-PE composites compared with unfilled PE and solid wood. We also evaluated the effect of five additive-type FRs systems on fire performance[21] and selected three of the best-performing FR systems (WF-BR, WF-MH, and WF-APP) for weathering under ASTM D2565. The work presented here used consistent formulations, materials, and methodologies.

This study provides a baseline of fire performance of WPCs based on lightening, TGA/DSC, and cone calorimetry tests with exterior application in mind with weathering. It also demonstrates the changes in fire performance that can be obtained when various additive-type FRs are incorporated into WPCs. Although all FRs had a positive effect on fire performance of WPCs, it is interesting to note that the addition of WF alone into PE can dramatically improve the fire performance of PE. For example, incorporating 60% wood into PE lowered the peak HRR of PE by 76%. In comparison, incorporating 50% wood and 10% MH (the combination that improved peak HRR the most) decreased the peak HRR of PE by 84%. Based on these results MH and APP were identified as the most effective FRs for WPCs and whose bulk amounts do not leach out to affect flammability, with a note that APP may negatively impact mechanical properties.

This study gave rise to future considerations for improving WPCs. Further improvement may be possible by encapsulating WPC boards with special coating to prevent surface leaching. Another improvement suggested in the literature is nano-sizing the WF to increase charring and improve fire resistance. Finally, evaluating a combination of 5% of MH and 5% of APP for the 10% FR to determine if they act synergistically and improve both flammability and mechanical properties is recommended.

Acknowledgements

The authors wish to thank American Wood Fibers, Struktol Company of America, Rio Tinto Materials, and Albemarle Corporation for the gracious donation of materials.

Declaration of conflicting interests

The author(s) declared no potential conflicts of interest with respect to the research, authorship, and/or publication of this article.

Funding

The author(s) received no financial support for the research, authorship, and/or publication of this article.

ORCID iDs

Mark Anthony Dietenberger https://orcid.org/0000-0002-8497-4149
Charles Boardman https://orcid.org/0000-0002-9571-5601

References

1. Clemons C. Wood-plastic composites in the United States: the interfacing of two industries. *For Prod J* 2002; 52(6): 10–18.
2. Grand View Research. Wood plastic composites market size, share & trends analysis report by products (polyethylene, polypropylene, by application (automotive), by region, and segment forecasts, 2023-2030 [report ID:978-1-68038-849-7]. San Francisco, CA: Grand View Research, 2023, https://www.grandviewresearch.com/industry-analysis/wood-plastic-composites-market
3. Stark N, White R and Clemons C. Heat release rate of wood plastic composites. *SAMPE J* 1997; 33(5): 26–31.
4. White RH, Dietenberger MA and Stark NM. Cone calorimeter tests of wood-based decking materials. In: *Proceedings eighteenth annual BCC conference on flame retardancy*, Stamford, CT, 21–23 May 2007, pp. 326–337. Stamford, CT: BCC Research.
5. Seefeldt H and Braun U. A new flame retardant for wood materials tested in wood plastic composites. *Macromol Mater Eng* 2012; 297: 814–820.
6. Borysiak S, Paukszta D and Helwig M. Flammability of wood-polypropylene composites. *Polym Degrad Stab* 2006; 91(12): 3339–3343.
7. Chapple S and Anandjiwala R. Flammability of natural fiber-reinforced composites and strategies for fire retardancy: a review. *J Thermoplast Compos Mater* 2010; 23: 871–893.
8. Tshai KY and Kong I. Advancement in flame retardancy of natural fibre reinforced composites with macro to nanoscale particulates additives. In: Goh KL, Aswathi MK, De Silva RT, et al. (eds) *Interfaces in particle and fibre reinforced composites*. Sawston: Woodhead Publishing, 2020, pp. 311–342.
9. Sain M, Park SH, Suhara F, et al. Flame retardant and mechanical properties of natural fibre-PP composites containing magnesium hydroxide. *Polym Degrad Stab* 2004; 83(2): 363–367.
10. El-Sabbagh A, Steuernagel L and Ziegmann G. Low combustible polypropylene/flax/magnesium hydroxide composites: mechanical, flame retardation characterization and recycling effect. *J Reinf Plast Compos* 2013; 32: 1030–1043.
11. Shen KK and Olson E. The use of borates and talc as fire retardants in wood plastic composite. In: *Proceedings seventeenth annual BCC conference on flame retardancy*. Stamford, CT, 22–24 May 2006, pp. 289–296. Stamford, CT: BCC Research.
12. Ayrilmis N, Akbulut T, Dundar T, et al. Effect of boron and phosphate compounds on physical, mechanical, and fire properties of wood-polypropylene composites. *Constr Build Mater* 2012; 33: 63–69.
13. García M, Hidalgo J, Garmendia I, et al. Wood-plastic composites with better fire retardancy and durability performance. *Composites A* 2009; 40: 1772–1776.
14. Abu Bakar MB, Mohd Ishak ZA, Mat Taib R, et al. Flammability and mechanical properties of wood flour filled polypropylene composites. *J Appl Polym Sci* 2010; 116: 2714–2722.
15. Zhang ZX, Zhang J, Lu B-X, et al. Effect of flame retardants on mechanical properties, flammability, and foamability of PP/wood-fiber composites. *Composites B* 2012; 43: 150–158.
16. Li B and He J. Investigation of mechanical property, flame retardancy and thermal degradation of LLDPE-wood-fibre composites. *Polm Degrad Stab* 2004; 83(2): 241–246.
17. Kalali EN, Zhang L, Shabestari ME, et al. Flame-retardant wood polymer composites (WPCs) as potential fire safe bio-based materials for building products: preparation, flammability and mechanical properties. *Fire Saf J* 2019; 107: 210–216.
18. Krehula LK, Katančić Z, Marić G, et al. Study of fire retardancy and thermal and mechanical properties of HDPE-wood composites. *J Wood Chem Technol* 2015; 35: 412–423.
19. Pan M, Mei C, Du J, et al. Synergistic effect of nano silicon dioxide and ammonium polyphosphate on flame retardancy of wood fiber-polyethylene composites. *Composites A* 2014; 66: 128–134.
20. Arao Y, Nakamura S, Tomita Y, et al. Improvement on fire retardancy of wood flour/polypropylene composites using various fire retardants. *Polym Degrad Stab* 2014; 100: 79–85.
21. Stark NM, Mueller SA, White RH, et al. Evaluation of Various Fire Retardants for Use in Wood Flour/Polyethylene Composites. *Polym Degrad Stab* 2010; 95(9): 1903–1910.
22. Schirp A and Su S. Effectiveness of pre-treated wood particles and halogen-free flame retardants used in wood-plastic composites. *Polym Degrad Stab* 2016; 126: 81–92.
23. Schirp A and Hellmannn A. Fire retardance improvement of high-density polyethylene composites based on thermomechanical pulp treated with ammonium polyphosphate. *Polym Compos* 2019; 10: 2410–2423.
24. Braun U, Wachtendorf V, Geburtig A, et al. Weathering resistance of halogen-free flame retardance in thermoplastics. *Polym Degrad Stab* 2010; 95: 2421–2429.
25. Vahabi H, Sonnier R and Ferry L. Effects of ageing on the fire behaviour of flame-retarded polymers. *Polym Int* 2015; 64: 313–328.
26. Stark NM and Matuana LM. Effect of processing method on surface and weathering characteristics of wood-flour/HDPE composites. *J Appl Polym Sci* 2004; 93(3): 1021–1030.
27. Schirp A and Schwarz B. Influence of compounding conditions, treatments of wood particles with fire-retardants and artificaial weathering on properties of wood-polymer composites for façade applications. *Eur J Wood Wood Prod* 2021; 79: 821–840.
28. Lyon RE.Chapter 11 solid state thermochemistry of flaming combustion. In: Grand AF and Wilkie CA (eds) *Fire retardancy of polymeric materials*. New York: Marcel Dekker, Inc., 2000, pp. 391–447.
29. Georlette P, Simons J and Costa L.Halogen-containing fire-retardant compounds. In: Grand AF and Wilkie CA (eds) *Fire retardancy of polymeric materials*. New York: Marcel Dekker, Inc., 2000, p. 245.
30. Weil ED.Synergists, adjuvants, and antagonists in flame-retardant systems. In: Grand AF and Wilkie CA (eds) *Fire retardancy of polymeric materials*. New York: Marcel Dekker, Inc., 2000, p. 115.
31. Green J.Phosphorous-containing flame retardants. In: Grand AF and Wilkie CA (eds) *Fire retardancy of polymeric materials*. New York: Marcel Dekker, Inc., 2000, p. 147.
32. Joseph P and Ebdon JR.Chapter 5 phosphorus-based flame retardants. In: Wilkie CA and Morgan AB (eds) *Fire retardancy of polymeric materials*. 2nd ed. Boca Raton, FL: CRC Press, 2010, pp. 107–127.
33. ASTM D7032:2021. Standard specification for establishing performance ratings for wood-plastic composite and plastic lumber deck boards, stair treads, guards, and handrails.
34. ASTM Standard D 2898. *Annual book of ASTM standards* (8.01). Conshocken, PA: American Society for Testing and Materials, 2008.
35. ASTM D2565:2023. Standard practice for xenon-arc exposure of plastics intended for outdoor applications.

36. Tang WK and Eickner HW. *Effect of inorganic salts on pyrolysis of wood, cellulose, and lignin determined by differential thermal analysis*. USDA Forest Service research paper FPL 82, January 1968. Washington, DC: USDA Forest Service
37. Rowell RM and Dietenberger MA. Chapter 6. Thermal properties, combustion, and fire retardancy of wood. In: Rowell R (ed.) *Handbood of wood chemistry and wood composites*. 2nd ed. Boca Raton, FL: CRC Books, 2013, pp. 127–149, https://www.fs.usda.gov/research/treesearch/41925
38. Cordeiro I, Chen T, Yuen A, et al. Pyrolysis and combustion characterization of HDPE/APP composites via molecular dynamics and CFD simulations. *J Anal Appl Pyrolysis* 2022; 163: 105499.
39. ASTM D2244:2023. Standard practice for calculation of color tolerances and color differences from instrumentally measured color coordinates.
40. ASTM E1354:2023. Standard test method for heat and visible smoke release rates for materials and products using and oxygen consumption calorimeter.
41. ASTM E 2102:2021. Standard test method for measurement of mass loss and ignitability for screening purposes using a conical radiant heater.
42. AS 3959. Construction of Buildings in Brushfire Prone Areas - Western Australia. (Standards Australia 2018c).
43. SFM 12-7A-4. Materials and Construction Methods for Exterior Wildfire Exposure - Decking SFM Standard. (California State Fire Marshall 2016).
44. White R, Stark N and Avrilmis N. Recent activities in flame retardancy of wood-plastic composites at the Forest Products Laboratory. In: *22nd annual conference on recent advances in flame retardancy of polymeric materials*, Stamford, CT, 23–25 May 2011.
45. Stark N. Considerations in the weathering of wood-plastic composites. In: *Proceedings: 3rd wood fibre polymer composites international symposium: innovative sustainable materials applied to building and furniture*, Bordeaux, 26–27 March 2007.
46. Dietenberger MA. Pyrolysis kinetics and combustion of thin wood by an advanced cone calorimetry test method. *J Therm Anal Calorim* 2012; 109: 1215–1228, https://www.fs.usda.gov/research/treesearch/41242
47. Cho J, Davis JM and Huber GW. The intrinsic kinetics and heats of reactions for cellulose pyrolysis and char formation. *ChemSusChem* 2010; 3: 1162–1165.
48. Werner K, Pommer L and Broström M. Thermal decomposition of hemicelluloses. *J Anal Appl Pyrolysis* 2014; 110: 130–137.
49. Kuang K, Huang X and Liao G. A comparison between superfine magnesium hydroxide powders and commercial dry powders on fire suppression effectiveness. *Process Saf Environ Prot* 2008; 86: 182–188.
50. Fernandes VJ, Fernandes NS, Fonseca VM, et al. Kinetic evaluation of decabromodiphenil oxide as a flame retardant for unsaturated polyester. *Thermochim Acta* 2002; 388(1–2): 283–288.
51. Wu Y, Yao C, Hu Y, et al. Comparative performance of three magnesium compounds on thermal degradation behavior of red gum wood. *Materials* 2014; 7: 637–652.
52. Kandola BK and Horrocks RA. Complex char formation in flame-retarded fibre-intumescent combinations-II. Thermal analytical studies. *Polym Degrad Stab* 1996; 54: 289–303.
53. Dietenberger MA and Grexa O. Ignitability of materials in transitional heating regimes. In: *Wood & fire safety: proceedings, 5th international scientific conference*, Zvolen, 18–22 April 2004, pp. 31–41. Zvolen: Faculty of Wood Sciences and Technology, Technical University of Zvolen.
54. Dietenberger MA and White RH. Reaction-to-fire testing and modeling for wood products. In: *Proceedings, 12th annual BCC conference on flame retardancy*, Stamford, CT, 21–23 May 2001, pp. 54–69. Nonvalk, CT: Business Communications Co., Inc.
55. ASTM E84:2023c. Standard test method for surface burning characteristics of building materials.

Author biographies

Mark Dietenberger is a Research General Engineer at the Forest Products Laboratory. His research interests focus on Fire Safety Science for building products and for forest materials related to WUI.

Nicole M Stark is a Research Chemical Engineer at the Forest Products Laboratory. Her research interests focus on development of composites combining wood fibers or cellulose nanomaterials with other polymeric materials.

Charles Boardman is a General Engineer at the Forest Products Laboratory. His research interests focus on Building Science and instrumentation.